Biomedicine & Pharmacotherapy 118 (2019) 109228

Contents lists available at ScienceDirect

Biomedicine & Pharmacotherapy

journal homepage: www.elsevier.com/locate/biopha

Profiles of immune cell infiltration and immune-related genes in the tumor microenvironment of colorectal cancer

Penglei Ge[a,*], Weiwei Wang[b], Lin Li[a], Gong Zhang[a], Zhiqiang Gao[a], Zhe Tang[a], Xiaowei Dang[a], Yang Wu[a,*]

[a] Department of Hepatobiliary and Pancreatic Surgery, The First Affiliated Hospital of Zhengzhou University, No. 1 Jianshe East Road, Zhengzhou, Henan Province, China
[b] Department of Pathology, The First Affiliated Hospital of Zhengzhou University, No. 1 Jianshe East Road, Zhengzhou, Henan Province, China

ARTICLE INFO

Keywords:
Immune cell
Immune-related genes
Immunotherapy
Colorectal cancer
Tumor microenvironment

ABSTRACT

Purpose: tumor-infiltrating immune cells are highly relevant to the progression and prognosis of colorectal cancer (CRC). The aim of this study is to explore the immune cells and immune-related gene expression in tumor microenvironment of CRC.

Methods: CIBERSORT, a deconvolution algorithm, was used to analyze the infiltration of 22 immune cell types in the tumor microenvironment and immune-related gene expression in 404 CRC and 40 adjacent non-tumorous tissues.

Results: a wide heterogeneity of immune cells among different paired tissues and in tumor stages was uncovered. M0 macrophages, M1 macrophages and CD4 memory activated T cells were infiltrated significantly more in CRC compared with normal tissues in both TCGA and GEO cohorts. CRC with T1–2 tumor stage showed increased CD4 memory activated T cells compared with T3–4 tumors. M0 macrophages were the highest in stage N1 tumors. Significant immune-related genes were identified to build prognostic models by Cox regression analysis. The concordance index of the prognostic model for TNM stage I–II was 0.69, and 0.71 for stage III–IV. The AUC values for 1-, 3-, and 5-year survivals were 0.674, 0.773, 0.812 for TNM stage I–II, respectively, and 0.764, 0.782, 0.803 for stage III–IV, respectively.

Conclusion: these results could assist clinicians in selecting targets for immunotherapies and individualize treatment strategies for patients with CRC.

1. Introduction

Colorectal cancer (CRC) is the third leading cause of cancer-related mortality worldwide [1]. Surgical resection is currently the most effective therapy for CRC. However, approximately 80% of CRC patients show recurrence during the first 3 years [2]. The emergence of new chemotherapeutic drugs and regimens has improved the overall survival rate of CRC patients to some extent, but drug resistance has seriously reduced the prognostic outcome of patients. Thus, identifying other effective treatments is important for improving the survival rate of patients with CRC.

Immunotherapy has shown encouraging results as an emerging treatment for some cancers, especially for melanoma and breast cancer [3,4]. Tumor cells in the tumor microenvironment (TME) can directly invade surrounding tissues or metastasize through blood and lymphatic vessels, and the infiltrated cells can induce the host immune response by releasing cytokines, cytokine receptors and other factors, which directly or indirectly inhibit or promote the progression of tumor cells. Therefore, better understanding of the immune status of the TME and exploring the distribution and function of immune cells are critical to improve the efficacy of immunotherapy in cancer.

Significantly fewer immune cells infiltrate in CRC compared with other tumors [5]. Furthermore, due to the heterogeneity of tumors, the quantity and distribution of immune cells among different patients and

Abbreviations: CRC, colorectal cancer; TCGA, the cancer genome atlas; CIBERSORT, cell type identifcation by estimating relative subsets of RNA transcripts; CD4, cluster of differentiation 4; NK, natural killer; GO, gene ontology; GEO, gene expression omnibus; PBS, phosphate buffered saline; IHC, immunohistochemical; AOD, average optical density; IL, interleukin; EREG, epiregulin; CALCA, calcitonin-related polypeptide α; STC2, stanniocalcin 2; NTS, neurotensin; TILs, tumor infiltrating lymphocytes; CNS, central nervous system; EGFR, epidermal growth factor receptor

* Corresponding authors at: Department of Hepatobiliary and Pancreatic Surgery, The First Affiliated Hospital of Zhengzhou University, No. 1 Jianshe East Road, Zhengzhou, Henan Province, China.

E-mail addresses: doc677@126.com (P. Ge), sunny2000@yeah.net (Y. Wu).

https://doi.org/10.1016/j.biopha.2019.109228
Received 11 April 2019; Received in revised form 7 July 2019; Accepted 15 July 2019

even at different pathologic stages in the same patient are quite discrepant. Thus, the patient's immune cell infiltration status can be accurately obtained only by selecting a precise method to detect a large number of samples.

The cancer genome atlas (TCGA) contains a large amount of transcriptome data that can provide many samples. "Cell type Identifcation By Estimating Relative Subsets Of RNA Transcripts "(CIBERSORT) is a biology tool that uses the deconvolution method to analyze bulky gene expression data of 22 immune cell types, using a signature matrix of 547 marker genes in amount of heterogeneous samples, and then fractions of immune cells infiltrated in the TME can be obtained [6]. CIBERSORT has been successfully validated, and used for determining immune cell landscapes and their relations to treatment response and outcome in breast, lung and liver cancers [7–9].

Reliable prognostic biomarkers are needed to select patients at high risk for recurrence, as well as patients who should receive targeted surveillance and additional systemic therapy. To more precisely apply immunotherapy, the identification of immune-related genes is particularly critical. In this study, we identified immune-related genes of CRC and gene ontology (GO) was analyzed to reveal how these genes are involved in the immune response. Furthermore, two predictive models for TNM stage I–II and III–IV, characterized with only immune-related genes, were built to estimate disease prognosis and patient survival. The combination analysis of immune cells and immune-related genes provides a deeper understanding about the immune response of the TME in CRC.

2. Materials and methods

2.1. Data from the TCGA cohort

The transcriptome expression profiles and corresponding clinical information of colorectal adenomas and adenocarcinomas were downloaded from the Genomic Data Commons Data Portal of TCGA (https://cancergenome.nih.gov/). The expression data was HTSeq-FPKM type, containing 404 CRC tissues and 40 adjacent non-tumorous tissue samples as of January 2019.

2.2. Differentially expressed mRNAs between CRC and non-tumorous tissues

An expression profile of 23,113 RNAs in CRC was obtained from TCGA. The differentially expressed mRNA data were screened using edgeR package, with parameters of logFoldchange (FC) > 2 or < -2 and P value < 0.05. A total of 1820 differentially expressed mRNAs were used to filter in two subsequent analyses, including immune cell infiltration and immune-related genes.

2.3. Data from the GEO cohort

To ensure the accuracy of results from the TCGA cohort, Gene Expression Omnibus (GEO, https://www.ncbi.nlm.nih.gov/geo/) datasets were analyzed for validation. Publicly available raw microarray expression data of CRC was collected from GEO for eligible datasets. GSE21510, with Affymetrix Human Genome U133 Plus 2.0 microarray expression series matrix files and GPL570 platform, was selected. A total of 22,753 genes were collated, which included 123 CRC tissues and 25 adjacent non-tumorous tissues samples. Infiltrated immune cells were analyzed and compared with data from TCGA.

The data from TCGA and GEO were both publicly available and open access, so no approval was needed from the ethics committees.

2.4. Evaluation of immune cell infiltration

Tumor-infiltrating immune cells were calculated using the CIBERSORT algorithm [6]. CIBERSORT is an analytical tool, with a gene expression signature matrix of 547 marker genes, that is used for quantifying the infiltrated immune cell composition fractions. LM22 is the annotated gene signature matrix defining 22 immune cell subtypes and was downloaded from the CIBERSORT web portal (http://cibersort.stanford.edu/).

The 22 immune cells included seven types of T cells, naive B cells, memory B cells, plasma cells, resting NK cells, activated NK cells, monocytes, M0–M2 macrophages, resting dendritic cells, activated dendritic cells, resting mast cells, activated mast cells, eosinophils and neutrophils (Supplementary 1).

To improve the accuracy of the deconvolution algorithm, CIBERSORT p-value and root mean squared error were counted for each sample file. The algorithm used a default signature matrix at 100 permutations. Only data with CIBERSORT p-value < 0.05 were filtered and selected for the next analysis.

Immune cell fractions of all samples from both the TCGA and GEO cohorts were analyzed using the CIBERSORT algorithm.

2.5. Correlation analysis of tumor infiltrated immune cells and clinical information

Only samples with immune cell files in both the TCGA and GEO datasets meeting the filtering conditions were selected for the subsequent clinical analysis. The filtered immune cell expression matrix was merged with the clinical information matrix from TCGA. Survival analysis of the filtered immune cells and the correlations between the cells and tumor stages were evaluated.

2.6. Immunohistochemical validation of the three immune cells

From February 2014 to November 2015, 37 CRC patients who underwent curative resection and didn't receive neoadjuvant therapy before surgery at The First Affiliated Hospital of Zhengzhou University (Zhengzhou, China) participated in this study in accordance with the provisions of Helsinki Declaration. All haematoxylin and eosin stained slides of each tumor sample were examined and confirmed by two experienced pathologists. All formalin-fixed paraffin-embedded CRC samples were collected to examine the protein levels of the three infiltrated immune cells.

Slides with 4um sections from the paraffin-embedded specimens were deparaffinized and rehydrated. Heatmediated antigen retrieval was conducted in a steamer for 23 min. Endogenous peroxidase activity was blocked by incubating the sections with 3% hydrogen peroxide at room temperature for 25 min. After washing with phosphate buffered saline (PBS) three times and incubation with bovine serum at room temperature for 30 min, the slides were further incubated with primary antibodies overnight at 4 °C. Following a PBS wash, the slides were incubated with secondary antibody for 30 min. Then they were washed with PBS and incubated with 3.3′-diaminobenzidine solution for 5 min. Each section was counterstained with hematoxylin after washing with water. All immunohistochemical (IHC) slides were analyzed using Image-pro plus 6.0 software (Media Cybernetics, USA). The results were tested by two pathologists. For IL23A and CD68 expression analysis, the relevant primary antibodies (BS-18146R, 1:400; Bioss, and GB14043, 1:200; Servicebio) were used. IL23A and CD68 are both localized in the nucleus. The results were expressed with average optical density (AOD) for IL23A, and mean positive cell density per unit tissue for CD68.

2.7. Immune-related gene analysis of the TCGA cohort

A total of 1534 immune-related genes and GO were downloaded from the ImmPort database (https://immport.niaid.nih.gov) [10] (Supplementary 2), including antigen processing and presentation pathways, B cell receptor signaling pathway, cytokines, cytokine receptors, interleukins, NK cell cytotoxicity, transforming growth factor-β family member, T cell receptor signaling pathway, and TNF family

member receptors. The immune-related genes among the 1820 differentially expressed mRNAs in the TCGA cohort were identified. A total of 148 immune-related mRNAs were filtered for GO and clinical analysis.

2.8. Validation of the immune-related genes with the GEO cohort

To verify the differentially expressed immune-related genes from the TCGA cohort, we attempted to extract the expression of related genes from the GEO cohort (GSE21510) for further analysis. The differentially expressed profiles of the related genes between CRC and adjacent non-tumorous tissues were studied.

2.9. Statistical analysis

All analyses were conducted using R software (version 3.5.2). Only cases with CIBERSORT p-value < 0.05 were included in the subsequent analysis. The differential infiltrations of the 22 immune cell types in the TCGA and GEO cohorts were evaluated by Wilcox test. Correlations among different immune cells were tested by corrplot R package. Survival R package was used for Kaplan-Meier curve analysis. Wilcox test was performed to analyze correlations between filtered immune cells and TNM stage. Univariate and multivariate analyses were performed using Cox regression. Survival rate of ROC analysis was calculated by time ROC R package. Concordance index was assessed by survcomp R package. The two-tailed paired *t*-test was used for data of expression of IL23A and CD68. Validation of the immune-related genes between CRC and adjacent non-tumorous tissues in GEO cohort were studied using Wilcoxon signed-rank test. All statistical tests were two sided and p values < 0.05 were considered as statistically significant.

3. Results

3.1. Clinical characteristics

A flowchart of the analysis procedure for this study is shown in Fig. 1. A total of 388 patients diagnosed with CRC were registered in the TCGA cohort. To reduce the effect of surgery on short-term mortality, patients with survival time less than 30 days were deleted. A total of 364 patients remained, including 199 male (54.67%) and 165 female patients (45.33%). Detailed clinical characteristics of all patients are listed in Table 1.

Table 1
Clinical characteristics of patients with CRC in TCGA. NA, not available.

Variables	Case, N (%)
Age at diagnosis, y	
≤60	110 (30.22%)
> 60	254 (69.78%)
Gender	
Male	199 (54.67%)
Female	165 (45.33%)
Pathologic-stage	
I	65 (17.86%)
II	138 (37.91%)
III	98 (26.92%)
IV	52 (14.29%)
NA	11 (3.02%)
TNM-T	
T1	10 (2.75%)
T2	67 (18.41%)
T3	248 (68.13%)
T4	39 (10.71%)
TNM-N	
N0	217 (59.62%)
N1	85 (23.35%)
N2	62 (17.03%)
TNM-M	
M0	273 (75.00%)
M1	52 (14.29%)
NA	39 (10.71%)

3.2. Composition of immune cells in tumor and normal tissues in the TCGA cohort

We first investigated the fractions of infiltrated immune cells between paired tumor and adjacent non-tumorous tissues in the TCGA cohort. Among the total samples, 92 tumor and 8 normal samples were eligible with CIBERSORT p < 0.05. No significant fractions of CD4 naive T cells and gamma delta T cells were found in CRC and normal tissues. The expression signature matrix of the other 20 infiltrated immune cell types was analyzed. As shown in Fig. 2A–2C, the fractions of immune cells varied significantly among samples and groups. Activated mast cells, CD4 memory activated T cells and neutrophils were only expressed in tumor tissues and not significantly infiltrated in normal tissues. M0 macrophages, CD4 memory resting T cells, M2 macrophages, M1 macrophages, and naïve B cells represented the top five highest infiltrating fractions compared with other immune cells in CRC tissues. In normal tissues, the top five highest fractions of infiltrating

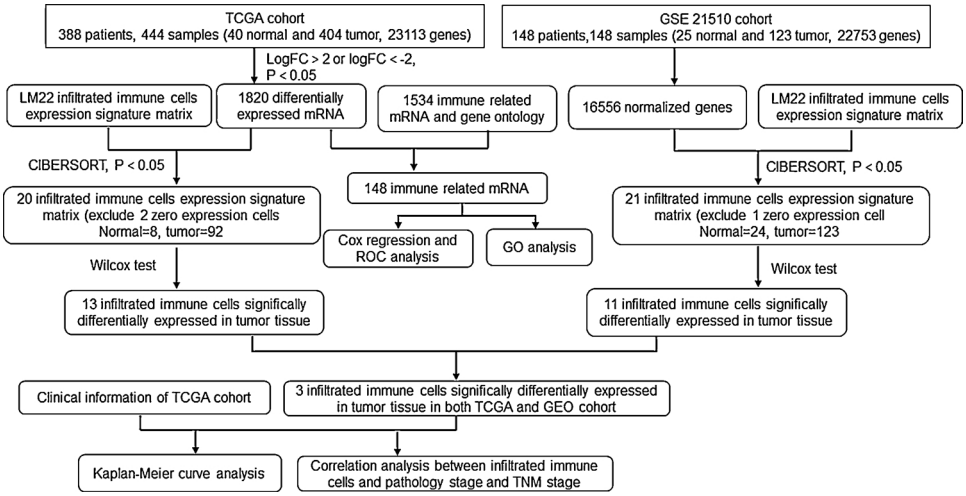

Fig. 1. Flowchart detailing the procedure of analyzing immune cells and their correlation with clinical characteristics, and prognostic models of immune-related genes.

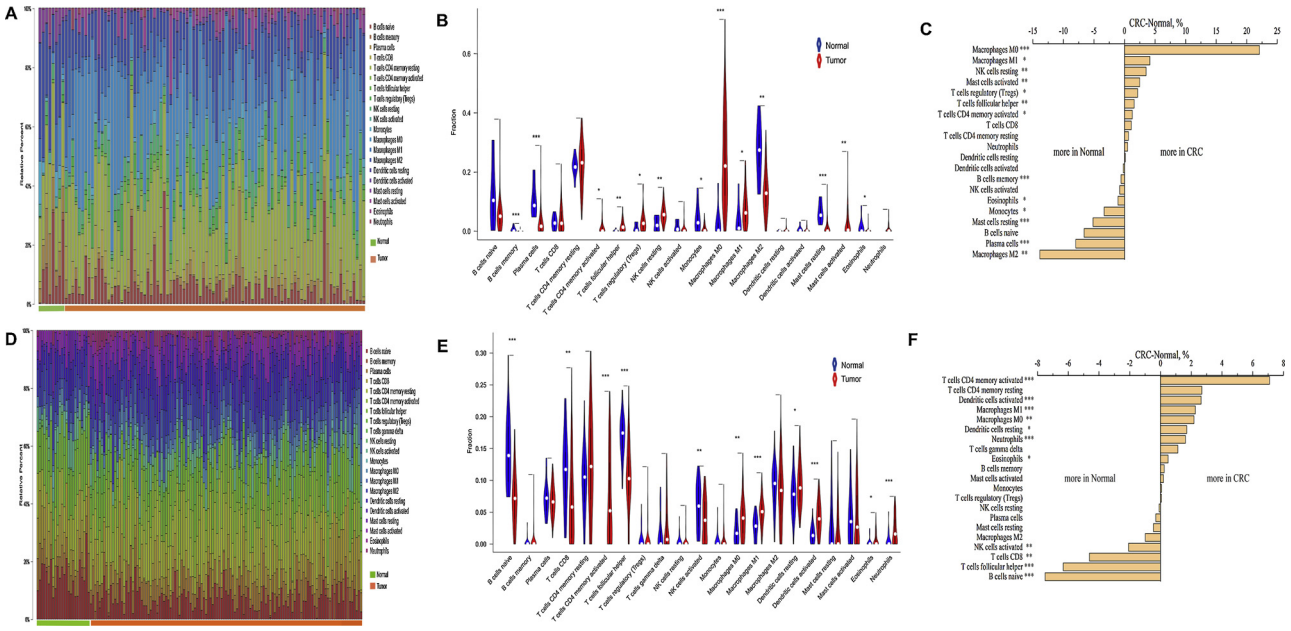

Fig. 2. Composition of infiltrated immune cells between paired tumor and adjacent normal tissues in the TCGA and GEO cohort with CIBERSORT $p < 0.05$ for all eligible samples. 20 immune cells in TCGA cohort and 21 immune cells in GEO cohort were filtered for analyzing. **(A)** Fractions of immune cells in 92 tumor and 8 normal samples in TCGA. **(B)** Comparisons of immune cells between tumor and normal tissues in TCGA. **(C)** Comparisons of immune cells more in tumor and more in normal tissues in TCGA. **(D)** Fractions of immune cells in 123 tumor and 24 normal samples in GEO. **(E)** Comparison of immune cells between tumor and normal tissues in GEO. **(F)** Comparison of immune cells more in tumor and more in normal tissues in GEO. *$p < 0.05$, **$p < 0.01$, ***$p < 0.001$.

Table 2
CIBERSORT fraction of 20 infiltrating immune cells in CRC and normal tissues in TCGA.

Immune cell type	Normal (%)	CRC (%)	P values
B cells naive	12.63 ± 11.21	6.01 ± 6.35	0.061
B cells memory	0.61 ± 0.96	0.03 ± 0.18	**< 0.001**
Plasma cells	10.74 ± 5.92	2.76 ± 4.27	**< 0.001**
T cells CD8	2.95 ± 2.28	4.06 ± 4.54	0.908
T cells CD4 memory resting	21.92 ± 3.57	22.56 ± 7.71	0.643
T cells CD4 memory activated	0	1.26 ± 2.39	**0.018**
T cells follicular helper	0.22 ± 0.40	1.80 ± 1.94	**0.008**
T cells regulatory (Tregs)	1.11 ± 1.47	3.25 ± 3.49	**0.033**
NK cells resting	2.36 ± 2.45	5.88 ± 3.11	**0.004**
NK cells activated	1.55 ± 1.84	0.76 ± 1.85	0.059
Monocytes	4.33 ± 5.03	1.00 ± 1.39	**0.023**
Macrophages M0	2.83 ± 5.57	24.90 ± 16.15	**< 0.001**
Macrophages M1	3.52 ± 5.61	7.65 ± 5.91	**0.021**
Macrophages M2	26.87 ± 9.93	13.02 ± 7.26	**0.001**
Dendritic cells resting	0.18 ± 0.29	0.31 ± 0.77	0.379
Dendritic cells activated	0.60 ± 1.08	0.39 ± 0.84	0.107
Mast cells resting	6.30 ± 3.37	1.14 ± 2.41	**< 0.001**
Mast cells activated	0	2.49 ± 4.25	**0.008**
Eosinophils	1.28 ± 3.00	0.21 ± 0.84	**0.039**
Neutrophils	0	0.51 ± 1.17	0.088

immune cells were M2 macrophages, CD4 memory resting T cells, naïve B cells, plasma cells, and resting mast cells. M0 macrophages were the most common infiltrated immune cell in CRC tissues compared with normal tissues ($p < 0.001$). Compared with normal tissues, CRC tissues also generally contained a higher fraction of M1 macrophages, resting NK cells, activated mast cells, regulatory T cells (Tregs), follicular helper T cells and CD4 memory activated T cells (all $p < 0.05$). The fraction of M2 macrophages was the lowest in tumor tissues compared with non-tumorous tissues ($p < 0.01$) (Table 2).

3.3. Composition of immune cells in tumor and normal tissues in the GEO cohort

To avoid the bias from only examining the TCGA cohort, we used GSE21510 as a validation dataset. After filtering with CIBERSORT $p < 0.05$, CD4 naive T cells were excluded, as they were not significantly expressed in both tumor and normal tissues in the Gene Expression Omnibus (GEO) dataset. A total of 21 immune cell types were analyzed in 123 tumor and 24 normal tissues. The most common immune cells in CRC tissues were CD4 memory resting T cells, follicular helper T cells, resting dendritic cells, M2 macrophages, and naive B cells. The immune cells with significantly higher fractions in tumor tissues compared with normal tissues were activated memory CD4 T cells, activated dendritic cells, M1 macrophages, M0 macrophages, dendritic cells, resting neutrophils and eosinophils (all $p < 0.05$). Naive B cells, follicular helper T cells, CD8 T cells, and activated NK cells were higher in normal tissues compared with tumor tissues (all $p < 0.05$) (Fig. 2D-2 F) (Table 3).

3.4. Correlation of significantly increased immune cells in tumor tissues in both the TCGA and GEO cohorts

We detected five immune cell types, including eosinophils, CD4 memory activated T cells, follicular helper T cells, M0 macrophages, and M1 macrophages, with significantly higher fractions in tumors than in normal tissues in both the TCGA and GEO cohorts. Among these five cell types, eosinophils and follicular helper T cells had opposite expression changes in the two cohorts. Thus, we selected CD4 memory activated T cells, M0 macrophages, and M1 macrophages for later analyses (Fig. 3A).

As shown in Fig. 3B, the fractions of different immune cells were weakly to moderately correlated in tumor tissues in the TCGA cohort. The five immune cells that showed the highest positive correlation with CD4 memory activated T cells were resting NK cells, CD8 T cells, M1 macrophages, follicular helper T cells and monocytes, while the five that showed the highest negative correlation were M0 macrophages, activated NK cells, resting mast cells, naive B cells and Tregs. In the validation with the GEO cohort, only M1 macrophages had a positive correlation and naive B cells and Tregs had a negative correlation with activated memory CD4 T cells (Fig. 3C).

Neutrophils showed a positive correlation with M0 macrophages in

Table 3
CIBERSORT fraction of 21 infiltrating immune cells in CRC and normal tissues in GEO.

Immune cell type	Normal (%)	CRC (%)	P values
B cells naive	14.61 ± 5.46	7.11 ± 4.15	< **0.001**
B cells memory	0.20 ± 0.74	0.44 ± 1.61	0.652
Plasma cells	7.13 ± 2.60	6.83 ± 2.37	0.775
T cells CD8	11.56 ± 5.99	6.94 ± 6.57	**0.001**
T cells CD4 memory resting	9.78 ± 5.10	12.47 ± 7.65	0.101
T cells CD4 memory activated	0	7.09 ± 6.90	< **0.001**
T cells follicular helper	16.83 ± 3.32	10.50 ± 5.17	< **0.001**
T cells regulatory (Tregs)	0.73 ± 1.64	0.79 ± 2.09	0.799
T cells gamma delta	1.60 ± 2.74	2.73 ± 3.80	0.138
NK cells resting	0.39 ± 0.99	0.30 ± 1.01	0.285
NK cells activated	6.02 ± 3.48	3.94 ± 3.25	**0.007**
Monocytes	0.49 ± 1.32	0.56 ± 1.27	0.768
Macrophages M0	1.95 ± 1.80	4.13 ± 3.06	**0.001**
Macrophages M1	2.79 ± 1.77	5.06 ± 2.23	< **0.001**
Macrophages M2	9.08 ± 3.65	8.09 ± 4.88	0.204
Dendritic cells resting	7.57 ± 3.38	9.28 ± 3.33	**0.034**
Dendritic cells activated	1.57 ± 1.40	4.21 ± 2.49	< **0.001**
Mast cells resting	2.90 ± 4.49	2.44 ± 3.36	0.854
Mast cells activated	4.03 ± 4.14	4.22 ± 4.68	0.912
Eosinophils	0.25 ± 0.68	0.74 ± 1.14	**0.011**
Neutrophils	0.51 ± 1.20	2.13 ± 2.18	< **0.001**

both the TCGA and GEO cohorts, but it was an extremely poor correlation. CD4 memory resting T cells and M2 macrophages had a moderate negative correlation with M0 macrophages in the TCGA cohort, which was validated in the GEO cohort.

The five immune cell types that showed the highest positive correlation with M1 macrophages in the TCGA cohort were follicular helper T cells, activated NK cells, CD4 memory resting T cells, CD4 memory activated T cells, and monocytes, and the five that showed a negative correlation with M1 macrophages were M0 macrophages, naïve B cells, activated mast cells, Tregs, plasma cells. In the validation in the GEO cohort, we found that follicular helper T cells, monocytes, and M0 macrophages showed the opposite correlation with that observed in the TCGA cohort.

3.5. Correlation of the three immune cells with survival rate, primary tumor and lymph node stage

We next examined immune cells with clinical information extracted from TCGA. Among M1 macrophages, M0 macrophages and CD4 memory activated T cells, only M1 macrophages could predict the survival rate. A high fraction of M1 macrophages was a risk factor ($p < 0.05$) (Fig. 4A).

Correlations of immune cells with primary tumor (T) stages and lymph node stages (N) were also assessed. The fraction of CD4 memory activated T cells was higher in T1–2 tumors than in T3–4 tumors ($p < 0.05$). M0 macrophage was highest in N1 tumors, and N2 tumors had the lowest fraction of M0 macrophages ($p < 0.05$) (Fig. 4B-4C).

3.6. Validation of the three immune cells

To validate the accuracy of results from TCGA and GEO datasets, we selected and tested clinical specimens from 37 CRC patients. The protein expressions of IL23A and CD68 which were respectively representative markers for CD4 memory activated T cells and macrophages were analyzed by quantitative IHC. Results showed a rise of IL23A in tumor tissues (1.09 ± 0.47) compared to adjacent non-tumorous tissues (0.86 ± 0.38) ($p < 0.05$). The positive cell density of CD68 was also higher in CRC tissues (26.22 ± 13.92) than that in normal tissues (22.62 ± 8.92) ($p < 0.05$) (Fig. 5).

3.7. GO and prognostic analysis of immune-related genes in TCGA cohort

The 148 immune-related genes examined in this study played various roles in immune functions. Most genes took effect of cytokines (54.05%) and cytokines receptors (21.62%) (Fig. 6G).

We divided TNM stage into stage I–II and stage III–IV to study the prognostic correlation of immune-related genes with different stages. In univariate Cox regression analysis of stage I–II, four genes, IL11, EREG, IL17C and CALCA (calcitonin-related polypeptide α), were selected for the multivariate Cox regression analysis to build a predictive model (Fig. 6A). The predictive model was characterized by the combination of expression levels of two genes evaluated by relative coefficient in multivariate Cox regression. The risk score was determined as follows: (0.1886 * expression level of IL11) + (-0.2060 * expression level of CALCA). It was a high risk predictive model with a concordance index of 0.69 (95% CI: 0.58–0.81) (Fig. 6B). The AUC values of 1-, 3-, and 5-year survival were 0.674, 0.773, and 0.812, respectively (Fig. 6E). In the forest map of univariate Cox regression analysis of stage III–IV, four significant genes were selected to build the multivariate Cox regression model (Fig. 6C). The score of the predictive model was determined as = (0.2904 * expression level of STC2) + (-0.1619 * expression level of EREG) + (0.1371 * expression level of NTS). The higher the score, the poorer the outcome was of the patient. The concordance index was 0.71 (95% CI: 0.62–0.80). The AUC values of 1-, 3-, and 5-year survival of the model were 0.764, 0.782, and 0.803, respectively (Fig. 6D, 6 F).

3.8. Validation of the immune-related gene expressions in stage I–II and III–IV with GEO database

In the TCGA cohort, IL11 and CALCA were highly expressed in CRC

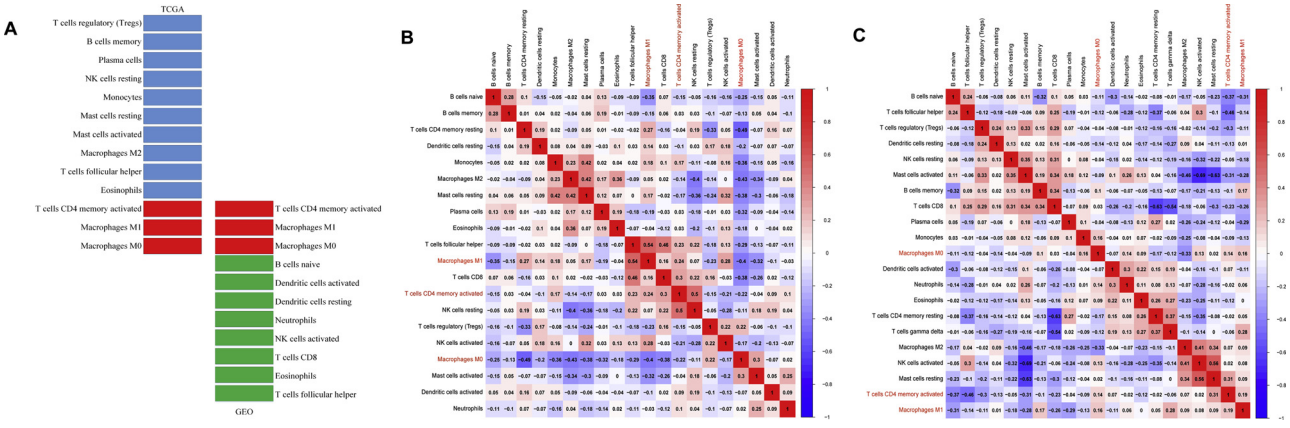

Fig. 3. (A) Red bars represented three significantly increased immune cells in tumor tissues in both TCGA and GEO cohorts. Correlation of CD4 memory activated T cells, M0 macrophages, M1 macrophages with other immune cells in TCGA **(B)** and in GEO **(C)**.

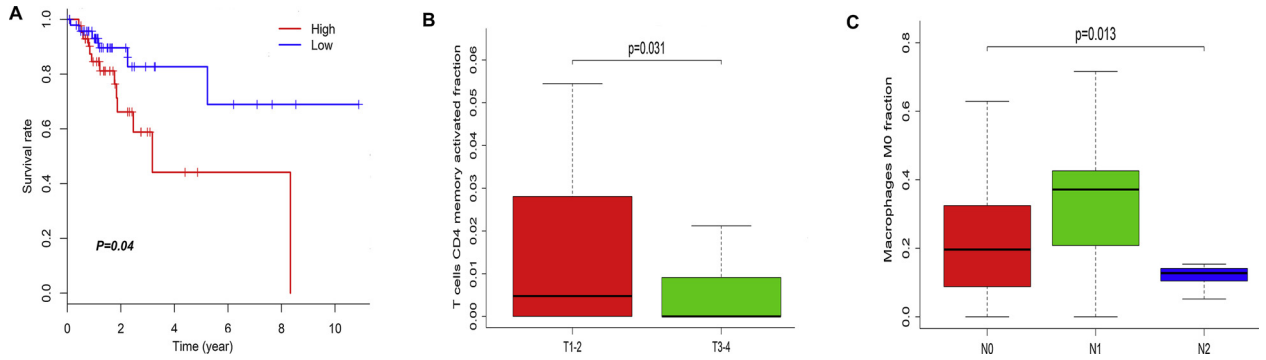

Fig. 4. (A) A high fraction of M1 macrophages was risk factor to predict survival rate in TCGA cohort. **(B)** Fraction of CD4 memory activated T cells was higher in T1–2 than in T3–4 tumors. **(C)** M0 macrophage was highest in N1 tumors.

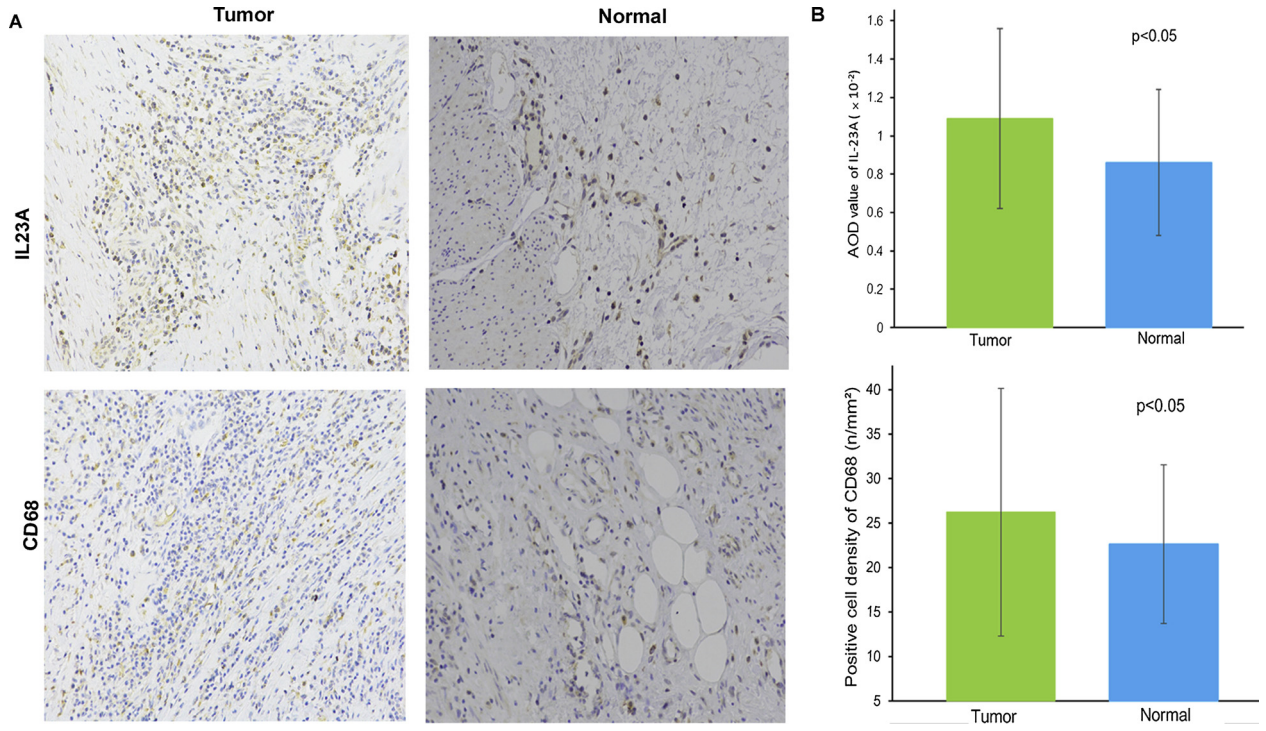

Fig. 5. Representative IHC stainings for **(A)** IL23A (CD4 memory activated T cells), CD68 (macrophages) in tumor tissue and adjacent non-tumorous tissues. AOD, average optical density. Magnification: 200 × . **(B)** Quantitative analysis of IL23A and CD68 in CRC and adjacent normal tissues.

compared with non-tumorous tissues in stage I–II. In the GEO database, only IL11 was expressed significantly higher in CRC tissues than in normal tissues, whereas CALCA showed no significant differences ($p > 0.05$). In stage III–IV of TCGA database, both STC2 and EREG were expressed higher and NTS was expressed lower in CRC than in normal tissues. In the validation in the GEO cohort, expressions of STC2 and EREG were consistent with those in TCGA, but NTS did not show significant differences between tumor and normal tissues ($p > 0.05$).

4. Discussion

The TME plays a critical role in tumor growth and progression [11,12] and consists of tumor cells and other surrounding non-tumor cells, such as immune cells and fibroblasts [13]. Tumor infiltrated immune cells are closely related to tumorigenesis, angiogenesis and the growth and metastasis of tumor cells, which could in turn regulate the quantity and defferentiate of immune cells [14]. Recent studies have revealed that tumor progression can result from imbalances between tumor progression and the host immune response [15]. Therefore, understanding the immune status and clarifying the amounts and functions of infiltrated immune cells in the TME may help lead to strategies to improve the response rate of immunotherapy.

In this study, we explored 22 infiltrated immune cell types in CRC tissues and adjacent non-tumorous tissues using the CIBERSOTR algorithm, and we examined the correlations of immune cells with clinical characteristics.

Marked differences in the immune cell composition were observed between CRC and normal intestinal tissues. Macrophages, both M0 and M1 subtypes, were the most infiltrated immune cells in tumor tissues compared with normal tissues. The most infiltrated immune cells in normal intestinal tissues compared with tumor tissues were also macrophages, but another subtype (M2). As the earlier and more amount infiltrated immune cells in TME, macrophages play an important role in tumor progression. Macrophages have different subtypes, which are differentiated under different cytokines. According to their activation, macrophages are divided into three subtypes (M0, M1 and M2), and each subtype serves different immune functions. M0 is the unactivated subtype and does not exhibit inflammatory or tumor-related function. Depending on the activation pathways, M0 can differentiate into two activated subtypes, M1 and M2, which each exhibit distinct

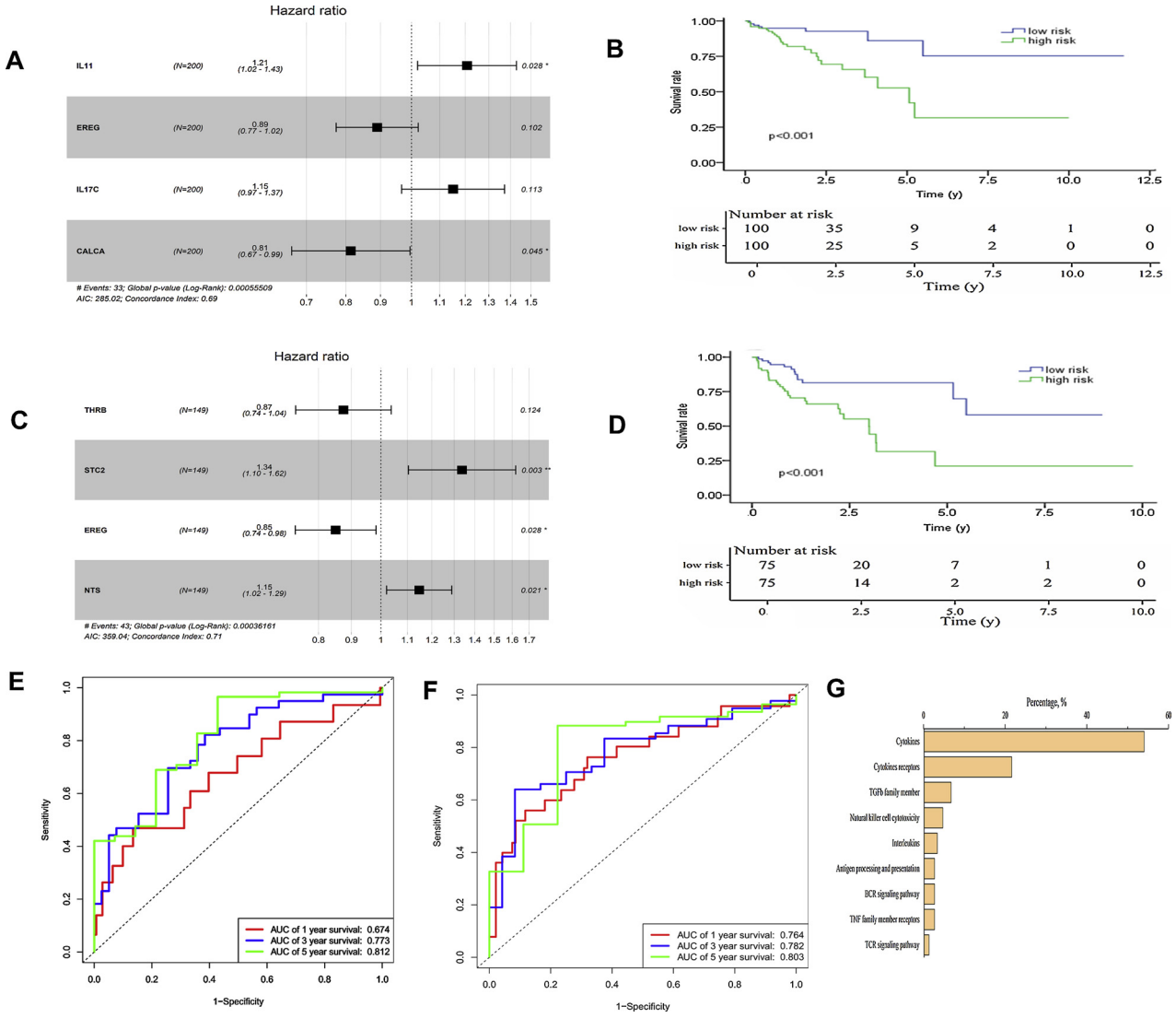

Fig. 6. (A) IL11 and CALCA were selected for multivariate Cox regression analysis to build a predictive model for stage I–II in TCGA. **(B)** Kaplan-Meier curve for prognostic model showing the overall survival based on relative high risk and low risk patients for stage I-II in TCGA. **(C)** STC2, EREG and NTS were selected to build a predictive model for stage III-IV in TCGA. **(D)** Kaplan-Meier curve for prognostic model for stage III-IV in TCGA. ROC curve analysis of survival prediction by the prognostic model for stage I-II **(E)** and stage III-IV **(F)** in TCGA. **(G)** GO analysis of 148 immune-related genes, with most genes taking effect of cytokines and cytokines receptors.

immunoregulatory roles. M1 macrophages secrete IL-12, IL-16, INF-γ and other pro-inflammatory cytokines to activate the inflammatory response and also participate in the host innate immunity, killing tumor cells in the TME. M2 macrophages mainly secrete cytokines such as IL-10 and TGF-β to inhibit inflammation; M2 macrophages are involved in Th2-type immune responses, inhibit T cell proliferation and differentiation, and promote proliferation of tumor cells and angiogenesis of tumor stroma. We found that more unactivated M0 macrophages and activated M1 macrophages infiltrated in CRC tissues compared with normal tissues, which was consistent with IHC result, indicating that tumor infiltrated macrophages play immune response functions and exhibit anti-tumor roles [16–21].

A previous study showed that tumor-associated macrophage infiltration of CRC tumors was correlated with a better outcome [22]. However, in survival analysis, we found that a high M1 macrophage fraction was a risk factor and indicated poor outcome. Macrophages had no significant correlation with pathologic stage ($p > 0.05$), but M0 macrophages had a significant correlation with lymph node stage. M0 macrophages had the highest fraction in N1 stage tumors, while N2 stage tumors showed the lowest fraction ($p < 0.05$). This result indicated that tumor infiltrated immune cells varied in different tumor stages and exhibit complex functions in tumor progression.

Tumor infiltrating lymphocytes (TILs), including T cells, B cells and NK cells, are another important component of immune cells that exhibit anti-tumoral functions, especially CD8+ and CD4 + T cells. Some studies showed that cytotoxic T cells, memory T cells and TH1 cells were associated with prolonged survival [23,24]. TILs are highly heterogeneous in intra-tumor and para-tumor areas, and in some cases even had opposite functions and effects on survival [25]. Studies in CRC showed that immune cells had a better prognostic predictive value than TNM stage, and tumor progression was significantly dependent on host cytotoxic and memory T cell density, a higher of which had a better outcome than others [26–28].

In our study, only CD4+ memory activated T cells among TILs significantly infiltrated in tumors, but these were less frequently observed in normal tissues. In survival analysis, CD4+ memory activated T cells had no relationship with survival time. In correlation analysis of immune cells and clinicopathological stages, CD4+ memory activated T cells had no correlation with all T-stage. However, we divided cases into T1–2 and T3–4, we found that the fraction of CD4+ memory

activated T cells was higher in T1–2 tumors than T3–4 tumors. This indicates that CD4+ memory activated T cells mainly infiltrated and anti-tumor in early stage of tumor progression.

Although other immune cells were significantly expressed in the TCGA cohort or GEO cohort, we focused on the immune cells significantly expressed in both cohorts to reduce bias of the results. The immune response is a complex process in which various immune cells play different roles and interact with each other. Tumor heterogeneity is obvious not only among individuals, but also at different tumor stages and in tumor sites. The types and degrees of infiltrated immune cells were largely different even in intra-tumor sites. Only by clarifying the infiltration of immune cells inside TME as much as possible can effective immunological treatment methods be identified for patients. To better understand the immune status of CRC, we further studied the expression of immune-related genes and the relationship with clinical survival and prognosis.

GO analysis of immune-related genes revealed that most genes played roles of cytokines and cytokines receptors. Cytokines are mainly expressed by immune cells and tumor cells in the TME. Cytokines are not only products of immune cells but also serve as information carriers between tumors and immune cells to influence changes in tumor immunity. Cytokines exhibit a range of characteristics, from anti-tumor to pro-tumor functions. These cytokines can directly or indirectly affect tumor cells in the TME through chronic inflammatory reactions, free radicals and signal pathways. Immune-related cytokine receptors exhibit a corresponding immune function by binding to relevant cytokines. Other immune-related genes exhibit various effects in different immune response phases in tumor occurrence and development, in antigen processing and presentation, as interleukins, and in NK cell cytotoxicity [29]. Future studies might uncover therapeutic directions for tumor immunotherapy by clarifying the mechanisms of cytokines.

All the differentially expressed immune-related genes were screened, and univariate and multivariate Cox analyses were conducted to build risk models to predict CRC I—II and III–IV stage prognosis. Two genes, IL11 and CALCA, were identified in stage I—II. High expression level of IL11 was relevant to a poor prognosis (HR 1.21, 95%CI = 1.02–1.43), and CALCA was correlated with a good prognosis (HR 0.81, 95%CI = 0.67–0.99). The AUCs of the ROC curve for the prognostic model for predicting the 1, 3 and 5- year survival were 0.674, 0.773 and 0.812, respectively, indicating that the two-gene signature had a good performance for survival prediction in CRC stage I—II patients. Patients were divided into high-risk group and low-risk group with the two immune-related gene based risk scoring model. According to the principle of individualized treatment, patients in each group should be managed with different strategies; patients in the high-risk group should receive more frequent tests to monitor recurrence and receive more targeted treatment.

Three genes were selected to construct a prognostic predictive model for stage III–IV. STC2 (Stanniocalcin 2) and NTS (neurotensin) are two risk immune-related genes and EREG (epiregulin) is a protective gene. The predictive model divided patients into high-risk and low-risk groups based on risk scores in CRC stage III–IV. In clinical practice, we distinguish patients with tumors into different groups using various clinicopathological stage criteria, with the aim of administering individualized treatments. Although patients with stage III–IV show mid- and late-stage tumors, we still hoped to further differentiate these patients through a model because of the individual differences in patients and tumor heterogeneity. Most patients in the high-risk group die in the first two years post-operation, so patients in this group should receive extremely frequent follow-up and be treated differently with conventional management.

STC2 is a glycoprotein as hormones to regulate calcium and phosphate secretion, exhibits potent growth-suppressive properties and participates in bone development [30,31]. STC2 is highly expressed in invasive breast cancer, hepatocellular carcinoma, prostate cancer, and CRC [32–35]. Chen et al. found that the average expression of STC2 in CRC tissues with TNM III–IV stages was 1.5-fold higher than TNM I–II stage CRC, and overall survival among patients with low STC2 expression in tumor tissues was longer compared with patients with high STC2 expression. The mechanism might involve STC2, as a cytokine, interacting with tyrosine kinase receptor to promote epithelial-mesenchymal transition and tumor metastasis [35].

NTS is a vasoactive peptide originally isolated from the brain [36]. NTS stimulates rodent mast cells to secrete histamine and increase histamine levels in plasma through the neurotensin receptor. NTS is also degraded by mast cell proteases, which inhibits its activity [37,38]. NTS is localized to neurons of the central nervous system (CNS) and endocrine cells of the gastrointestinal tract. As a hormone or neurotransmitter, NTS has two subtypes, the high-affinity NTS1 and the low-affinity NTS2, which exerts its effects primarily through specific G protein-coupled receptors. NTS1 is expressed in various regions of the CNS: small and large intestine, liver, and various cancers. NTS2 is located more diffusely in the CNS than NTS1 and is not expressed in the gastrointestinal tract. NTS stimulates growth and prevented apoptosis in gut mucosa, pancreatic acinar cells, and epithelial-based malignancies that express neurotensin receptors [39]. NTS is mainly distributed along the gastrointestinal tract and functions to decrease gastric motility, increase pancreaticobiliary secretion, facilitate fatty acid absorption, and increase the proliferation of normal intestinal mucosa [40–42]. Moreover, NTS promotes the growth of cancers, such as breast, prostate, pancreas, lung and gastrointestinal cancers [39,43,44].

EREG, together with amphiregulin, are ligands of the epidermal growth factor receptor (EGFR) tyrosine kinase family [45]. EREG can stimulate EGFR through an autocrine loop with positive feedback, and elevated EREG may indicate tumor dependence on the EGFR pathway [46]. Yoshida et al. found that high EREG in combination with other EGFR ligand expression predicted improved disease control and progression free survival [47]. EREG and its family members are crucially involved in tissue-specific proliferation and differentiation homeostasis. EREG proteins typically act in an autocrine and paracrine manner on specific cell membrane receptors and added an effective reparative response to any attack to biophysical integrity. Increasing evidence has indicated that the EGFR pathway can impact the inflammatory and immune reactions of the skin by enhancing the innate immune defense and overactivating keratinocyte pro-inflammatory functions [48]. Shirasawa et al. revealed that EREG might play a critical role in both lipopolysaccharide- and peptidoglycan-induced pro-inflammatory cytokine production in macrophages [49].

Immunotherapies are effective and promising for some tumor patients. However, previous studies suggested that CRC may not be suitable for immunotherapy compared with breast cancer and melanoma [50]. Our study uncovered that different immune cells infiltrated in both tumor and adjacent non-tumorous tissues in CRC, and macrophages were the most frequent infiltrating immune cells in tumor tissues. Among all the significant immune-related genes in the TME of CRC, most made different roles in immune response as cytokines and cytokines receptors. This study described the expression of immune cells and immune-related genes in the TME of CRC, laying the foundation for future exploration of tumor immunotherapy.

There were several limitations of our study. The first limitation is the small numbers of filtered samples for immune cell analysis with the CIBERSORT algorithm in the TCGA cohort. Second, the predictive models of stage I—II and III–IV did not perform external validation in the GEO cohort because GSE21510 lacked clinical data, so the models need further validation in large sample clinical studies. Third, the population race was mostly either white or not reported in the TCGA database, and thus these results can not be directly extrapolated to other racial groups.

In summary, we revealed the levels of 22 immune cells infiltrated in the TME of CRC and their associations with clinical outcome. The significant immune-related genes were also selected to built prognostic models for TNM stages and to explore their relationship with

pathological stages. These findings could assist clinicians in selecting targets for immunotherapies and individualize treatment strategies for patients with CRC.

Funding

This research received no external funding.

Declaration of Competing Interest

None.

Acknowledgement

We thank Edanz Group (www.edanzediting.com/ac) for editing a draft of this manuscript.

Appendix A. Supplementary data

Supplementary material related to this article can be found, in the online version, at doi:https://doi.org/10.1016/j.biopha.2019.109228.

References

[1] R.L. Siegel, K.D. Miller, A. Jemal, Cancer statistics, CA Cancer J. Clin. 68 (2018) (2018) 7–30, https://doi.org/10.3322/caac.21442.
[2] K.M. Augestad, M.A. Merok, D. Ignatovic, Tailored treatment of colorectal cancer: surgical, molecular, and genetic considerations, Clin. Med. Insights Oncol. 11 (2017) 1–10, https://doi.org/10.1177/1179554917690766.
[3] R.J. Sullivan, K.T. Flaherty, Immunotherapy: Anti-PD-1 therapies-a new first-line option in advanced melanoma, Nat. Rev. Clin. Oncol. 12 (2015) 170–171, https://doi.org/10.1038/nrclinonc.2015.170.
[4] F.J. Esteva, V.M. Hubbard-Lucey, J. Tang, L. Pusztai, Immunotherapy and targeted therapy combinations in metastatic breast cancer, Lancet Oncol. 20 (2019) 175–186, https://doi.org/10.1016/S1470-2045(19)30026-9.
[5] K. Strasser, H. Birnleitner, A. Beer, D. Pils, M.C. Gerner, K.G. Schmetterer, T. Bachleitner-Hofmann, A. Stift, M. Bergmann, R. Oehler, Immunological differences between colorectal cancer and normal mucosa uncover a prognostically relevant immune cell profile, Oncoimmunology 8 (2019) e1537693, , https://doi.org/10.1080/2162402X.2018.1537693.
[6] A.M. Newman, C.L. Liu, M.R. Green, A.J. Gentles, W. Feng, Y. Xu, C.D. Hoang, M. Diehn, A.A. Alizadeh, Robust enumeration of cell subsets from tissue expression profles, Nat. Meth. 12 (2015) 453–457, https://doi.org/10.1038/nmeth.3337.
[7] R.D. Bense, C. Sotiriou, M.J. Piccart-Gebhart, J.B.A.G. Haanen, M.A.T.M. van Vugt, E.G.E. de Vries, C.P. Schroder, R.S.N. Fehrmann, Relevance of tumor-infiltrating immune cell composition and functionality for disease outcome in breast cancer, J. Natl. Cancer Inst. 109 (2016) 1–9, https://doi.org/10.1093/jnci/djw192.
[8] N. Rohr-Udilova, F. Klinglmüller, R. Schulte-Hermann, J. Stift, M. Herac, M. Salzmann, F. Finotello, G. Timelthaler, G. Oberhuber, M. Pinter, T. Reiberger, E. Jensen-Jarolim, R. Eferl, M. Trauner, Deviations of the immune cell landscape between healthy liver and hepatocellular carcinoma, Sci. Rep. 8 (2018) 6220–6230, https://doi.org/10.1038/s41598-018-24437-5.
[9] B. Chen, M.S. Khodadoust, C.L. Liu, A.M. Newman, A.A. Alizadeh, Profiling tumor infiltrating immune cells with CIBERSORT, Methods Mol. Biol. 1711 (2018) 243–259, https://doi.org/10.1007/978-1-4939-7493-1_12.
[10] S. Bhattacharya, S. Andorf, L. Gomes, P. Dunn, H. Schaefer, J. Pontius, P. Berger, V. Desborough, T. Smith, J. Campbell, E. Thomson, R. Monteiro, P. Guimaraes, B. Walters, J. Wiser, A.J. Butte, ImmPort: disseminating data to the public for the future of immunology, Immunol. Res. 58 (2014) 234–239, https://doi.org/10.1007/s12026-014-8516-1.
[11] D.F. Quail, J.A. Joyce, Microenvironmental regulation of tumor progression and metastasis, Nat. Med. 19 (2013) 1423–1437, https://doi.org/10.1038/nm.3394.
[12] J.A. Joyce, J.W. Pollard, Microenvironmental regulation of metastasis, Nat. Rev. Cancer 9 (2009) 239–252, https://doi.org/10.1038/nrc2618.
[13] Y.Z. Lim, A.P. South, Tumour-stroma crosstalk in the development of squamous cell carcinoma, Int. J. Biochem. Cell Biol. 53 (2014) 450–458, https://doi.org/10.1016/j.biocel.2014.06.012.
[14] M.L. Taddei, E. Giannoni, G. Comito, P. Chiaruqi, Microenvironment and tumor cell plasticity: an easy way out, Cancer Lett. 341 (2013) 80–96, https://doi.org/10.1016/j.canlet.2013.01.042.
[15] J. Galon, H.K. Angell, D. Bedognetti, F.M. Marincola, The continuum of cancer immunosurveillance: prognostic, predictive, and mechanistic signatures, Immunity. 39 (2013) 11–26, https://doi.org/10.1016/j.immuni.2013.07.008.
[16] A. Mantovani, A. Sica, M. Locati, Macrophage polarization comes of age, Immunity. 23 (2005) 344–346, https://doi.org/10.1016/j.immuni.2005.10.001.
[17] D.A. Hume, The many alternative faces of macrophage activation, Front. Immunol. 6 (2015) e370, https://doi.org/10.3389/fimmu.2015.00370.
[18] S. Gordon, Alternative activation of macrophages, Nat. Rev. Immunol. 3 (2003) 23–35, https://doi.org/10.1038/nri978.
[19] J.W. Pollard, Tumour-educated macrophages promote tumour progression and metastasis, Nat. Rev. Cancer 4 (2004) 71–78, https://doi.org/10.1038/nrc1256.
[20] L. Bingle, N.J. Brown, C.E. Lewis, The role of tumour-associated macrophages in tumour progression: implications for new anticancer therapies, J. Pathol. 196 (2002) 254–265, https://doi.org/10.1002/path.1027.
[21] Y. Xiong, K. Wang, H. Zhou, L. Peng, W. You, Z. Fu, Profiles of immune infiltration in colorectal cancer and their clinical significant: a gene expression-based study, Cancer Med. 7 (2018) 4496–4508, https://doi.org/10.1002/cam4.1745.
[22] M.J. Cavnar, S. Turcotte, S.C. Katz, D. Kuk, M. Gönen, J. Shia, P.J. Allen, V.P. Balachandran, M.I. D'Angelica, T.P. Kingham, W.R. Jarnagin, R.P. DeMatteo, Tumor-associated macrophage infiltration in colorectal cancer liver metastasis is associated with better outcome, Ann. Surg. Oncol. 24 (2017) 1835–1842, https://doi.org/10.1245/s10434-017-5812-8.
[23] M.L. Ascierto, V. De Giorgi, Q. Liu, D. Bedognetti, T.L. Spivey, D. Murtas, L. Uccellini, B.D. Ayotte, D.F. Stroncek, L. Chouchane, M.H. Manjili, E. Wang, F.M. Marincola, An immunologic portrait of cancer, J. Transl. Med. 9 (2011) 146, https://doi.org/10.1186/1479-5876-9-146.
[24] F. Pagès, J. Galon, M.C. Dieu-Nosjean, E. Tartour, C. Sautès-Fridman, W.H. Fridman, Immune infiltration in human tumors: a prognostic factor that should not be ignored, Oncogene 29 (2010) 1093–1102, https://doi.org/10.1038/onc.2009.416.
[25] W.H. Fridman, F. Pages, C. Sautes-Fridman, J. Galon, The immune contexture in human tumours: impact on clinical outcome, Nat. Rev. Cancer 12 (2012) 298–306, https://doi.org/10.1038/nrc3245.
[26] J. Galon, A. Costes, F. Sanchez-Cabo, A. Kirilovsky, B. Mlecnik, C. Lagorce-Pagès, M. Tosolini, M. Camus, A. Berger, P. Wind, F. Zinzindohoué, P. Bruneval, P.H. Cugnenc, Z. Trajanoski, W.H. Fridman, F. Pagès, Type, density, and location of immune cells within human colorectal tumors predict clinical outcome, Science 313 (2006) 1960–1964, https://doi.org/10.1126/science.1129139.
[27] B. Mlecnik, M. Tosolini, A. Kirilovsky, A. Berger, G. Bindea, T. Meatchi, P. Bruneval, Z. Trajanoski, W.H. Fridman, F. Pagès, J. Galon, Histopathologic-based prognostic factors of colorectal cancers are associated with the state of the local immune reaction, J. Clin. Oncol. 29 (2011) 610–618, https://doi.org/10.1200/JCO.2010.30.5425.
[28] F. Pagès, A. Kirilovsky, B. Mlecnik, M. Asslaber, M. Tosolini, G. Bindea, C. Lagorce, P. Wind, F. Marliot, P. Bruneval, K. Zatloukal, Z. Trajanoski, A. Berger, W.H. Fridman, J. Galon, In situ cytotoxic and memory T cells predict outcome in patients with early-stage colorectal cancer, J. Clin. Oncol. 27 (2009) 5944–5951, https://doi.org/10.1200/JCO.2008.19.6147.
[29] H.W. Chung, J.B. Lim, Role of the tumor microenvironment in the pathogenesis of gastric carcinoma, World J. Gastroenterol. 20 (2014) 1667–1680, https://doi.org/10.3748/wjg.v20.i7.1667.
[30] A.D. Gagliardi, E.Y. Kuo, S. Raulic, G.F. Wagner, G.E. DiMattia, Human stanniocalcin-2 exhibits potent growth-suppressive properties in transgenic mice independently of growth hormone and IGFs, Am. J. Physiol. Endocrinol. Metab. 288 (2005) 92–105, https://doi.org/10.1152/ajpendo.00268.2004.
[31] C.R. McCudden, K.A. James, C. Hasilo, G.F. Wagner, Characterization of mammalian stanniocalcin receptors mitochondrial targeting of ligand and receptor for regulation of cellular metabolism, J. Biol. Chem. 277 (2002) 45249–45258, https://doi.org/10.1074/jbc.M205954200.
[32] S. Esseghir, A. Kennedy, P. Seedhar, A. Nerurkar, R. Poulsom, J.S. Reis-Filho, C.M. Isacke, Identification of NTN4, TRA1, and STC2 as prognostic markers in breast cancer in a screen for signal sequence encoding proteins, Clin. Cancer Res. 13 (2007) 3164–3173, https://doi.org/10.1158/1078-0432.CCR-07-0224.
[33] H. Wang, K. Wu, Y. Sun, Y. Li, M. Wu, Q. Qiao, Y. Wei, Z.G. Han, B. Cai, STC2 is upregulated in hepatocellular carcinoma and promotes cell proliferation and migration in vitro, BMB Rep. 45 (2012) 629–634, https://doi.org/10.5483/bmbrep.2012.45.11.086.
[34] K. Tamura, M. Furihata, S.Y. Chung, M. Uemura, H. Yoshioka, T. Iiyama, S. Ashida, Y. Nasu, T. Fujioka, T. Shuin, Y. Nakamura, H. Nakagawa, Stanniocalcin 2 overexpression in castration-resistant prostate cancer and aggressive prostate cancer, Cancer Sci. 100 (2009) 914–919, https://doi.org/10.1111/j.1349-7006.2009.01117.x.
[35] B. Chen, X. Zeng, Y. He, X. Wang, Z. Liang, J. Liu, P. Zhang, H. Zhu, N. Xu, S. Liang, STC2 promotes the epithelial-mesenchymal transition of colorectal cancer cells through AKT-ERK signaling pathways, Oncotarget 7 (2016) 71400–71416, https://doi.org/10.18632/oncotarget.12147.
[36] B.M. Tyler-McMahon, M. Boules, E. Richelson, Neurotensin: peptide for the next millennium, Regul. Pept. 93 (2000) 125–136, https://doi.org/10.1016/s0167-0115(00)00183-x.
[37] A.M. Barrocas, D.E. Cochrane, R.E. Carraway, R.S. Feldberg, Neurotensin stimulation of mast cell secretion is receptor-mediated, pertussis-toxin sensitive and requires activation of phospholipase C, Immunopharmacology 41 (1999) 131–137, https://doi.org/10.1016/s0162-3109(98)00064-2.
[38] J. Donelan, W. Boucher, N. Papadopoulou, M. Lytinas, D. Papaliodis, P. Dobner, T.C. Theoharides, Corticotropin-releasing hormone induces skin vascular permeability through a neurotensin-dependent process, Proc. Natl. Acad. Sci. U. S. A. 103 (2006) 7759–7764, https://doi.org/10.1073/pnas.0602210103.
[39] W.C. Mustain, P.G. Rychahou, B.M. Evers, The role of neurotensin in physiologic and pathologic processes, Curr. Opin. Endocrinol. Diabetes Obes. 18 (2011) 75–82, https://doi.org/10.1097/MED.0b013e3283419052.
[40] B.M. Evers, Neurotensin and growth of normal and neoplastic tissues, Peptides 27 (2006) 2424–2433, https://doi.org/10.1016/j.peptides.2006.01.028.
[41] K. Kalafatakis, K. Triantafyllou, Contribution of neurotensin in the immune and neuroendocrine modulation of normal and abnormal enteric function, Regul. Pept.

170 (2011) 7–17, https://doi.org/10.1016/j.regpep.2011.04.005.
[42] J. Li, J. Song, Y.Y. Zaytseva, Y. Liu, P. Rychahou, K. Jiang, M.E. Starr, J.T. Kim, J.W. Harris, F.B. Yiannikouris, W.S. Katz, P.M. Nilsson, M. Orho-Melander, J. Chen, H. Zhu, T. Fahrenholz, R.M. Higashi, T. Gao, A.J. Morris, L.A. Cassis, T.W. Fan, H.L. Weiss, P.R. Dobner, O. Melander, J. Jia, B.M. Evers, An obligatory role for neurotensin in high-fat-diet-induced obesity, Nature 533 (2016) 411–415, https://doi.org/10.1038/nature17662.
[43] Z. Wu, D. Martinez-fong, J. Trédaniel, P. Forgez, Neurotensin and its high affinity receptor 1 as a potential pharmacological target in cancer therapy, Front. Endocrinol. (Lausanne) 3 (2013) 184–193, https://doi.org/10.3389/fendo.2012.00184.
[44] J.T. Kim, H.L. Weiss, B.M. Evers, Diverse expression patterns and tumorigenic role of neurotensin signaling components in colorectal cancer cells, Int. J. Oncol. 50 (2017) 2200–2206, https://doi.org/10.3892/ijo.2017.3990.
[45] M. Shoyab, V.L. McDonald, J.G. Bradley, G.J. Todaro, Amphiregulin: a bifunctional growth-modulating glycoprotein produced by the phorbol 12-myristate 13-acetatetreated human breast adenocarcinoma cell line MCF-7, Proc. Natl. Acad. Sci. U. S. A. 85 (1988) 6528–6532, https://doi.org/10.1073/pnas.85.17.6528.
[46] D.J. Jonker, C.S. Karapetis, C. Harbison, C.J. O'Callaghan, D. Tu, R.J. Simes, D.P. Malone, C. Langer, Epiregulin gene expression as a biomarker of benefit from cetuximab in the treatment of advanced colorectal cancer, Br. J. Cancer 110 (2014) 648–655, https://doi.org/10.1038/bjc.2013.753.
[47] M. Yoshida, T. Shimura, M. Sato, M. Ebi, T. Nakazawa, H. Takeyama, T. Joh, A novel predictive strategy by immunohistochemical analysis of four EGFR ligands in metastatic colorectal cancer treated with anti-EGFR antibodies, J. Cancer Res. Clin. Oncol. 139 (2013) 367–378, https://doi.org/10.1007/s00432-012-1340-x.
[48] S. Pastore, F. Mascia, V. Mariani, G. Girolomoni, The epidermal growth factor receptor system in skin repair and inflammation, J. Invest. Dermatol. 128 (2008) 1365–1374, https://doi.org/10.1038/sj.jid.5701184.
[49] S. Shirasawa, S. Sugiyama, I. Baba, J. Inokuchi, S. Sekine, K. Ogino, Y. Kawamura, T. Dohi, M. Fujimoto, T. Sasazuki, Dermatitis due to epiregulin deficiency and a critical role of epiregulin in immune-related responses of keratinocyte and macrophage, Proc. Natl. Acad. Sci. U. S. A. 101 (2004) 13921–13926, https://doi.org/10.1073/pnas.0404217101.
[50] A. Banerjea, S.A. Bustin, S. Dorudi, The immunogenicity of colorectal cancers with high-degree microsatellite instability, World J. Surg. Oncol. 3 (2005) 26–35, https://doi.org/10.1007/s10350-005-0203-9.